

## PI CONTROLLER DESIGN FOR TIME DELAY SYSTEMS USING DIFFERENT MODEL ORDER REDUCTION METHODS

Hilal İRGAN\*<sup>ID</sup>

Nusret TAN\*\*<sup>ID</sup>

Received: 22.06.2023; revised: 08.11.2023; accepted: 04.01.2024

**Abstract:** This study focuses on designing PI controllers for time-delay systems using various model order reduction techniques to reduce complexity. The stability boundary locus method was used to determine PI parameters that stabilizing reduced order models. After the PI parameters have been determined using the weighted geometric center method, the calculated controller parameters have been implemented in the original system. In this way, the efficiency of the controller design is effectively demonstrated through the reduction techniques. In addition, the study investigated the effectiveness of reduction methods with increasing time delay and adding an integrator to the system. The importance of these results is that they demonstrate the use of model order reduction techniques in the design of controllers for time-delay systems and reveal the advantages of these methods.

**Keywords:** Time-Delay, Weighted Geometrical Center, Model Order Reduction.

### Farklı Model Derecesi İndirgeme Yöntemleri Kullanılarak Zaman Gecikmeli Sistemler için PI Kontrolör Tasarımı

**Öz:** Bu çalışma, karmaşıklığı azaltmak için çeşitli model derecesi azaltma tekniklerini kullanarak zaman gecikmeli sistemlerde PI denetleyicileri tasarlamaya odaklanmıştır. Dereceleri azaltılmış modelleri stabilize eden PI parametrelerini belirlemek için kararlılık sınır eğrisi metodu kullanılmıştır. PI parametreleri ağırlıklı geometrik merkez yöntemi ile elde edildikten sonra, bu kontrolör parametreleri orijinal zaman gecikmeli modellerde uygulanmıştır. Böylece, model derecesi azaltma tekniklerinin uygulanması yoluyla kontrolör tasarımının verimliliği etkili bir şekilde gösterilmiştir. Ayrıca çalışma, artan zaman gecikmesi ve sisteme bir integratör eklenmesi ile model derecesi azaltma yöntemlerinin etkinliğini araştırmıştır. Bu bulguların önemi, zaman gecikmeli sistemlerde kontrolör tasarımında model derecesi azaltma tekniklerinin kullanımının gösterilerek bu yöntemlerin avantajlarının ortaya konmasıdır.

**Anahtar Kelimeler:** Zaman-Gecikmesi, Ağırlıklı Geometrik Merkez, Model Derecesi İndirgeme.

\* Tokat Gaziosmanpaşa University, Faculty of Engineering and Architecture, Department of Electrical and Electronics Engineering, Taşlıçiftlik Campus, 60250, Tokat

\*\* İnönü University, Faculty of Engineering, Department of Electrical and Electronics Engineering, 44280 Battalgazi/Malatya

Corresponding Author: Hilal İRGAN ([hilal.irgan@gop.edu.tr](mailto:hilal.irgan@gop.edu.tr))

**NOTE:** This article is an expanded version of the proceeding titled "PI Controller Design with Weighted Geometrical Center Method in Time Delay Systems Using Model Order Reduction Methods" which was presented orally at ELECO'2022 Conference and was invited by the conference organizing committee to be evaluated in Uludağ University Journal of The Faculty of Engineering (UJFE).

## 1. INTRODUCTION

In practice, many systems have a time delay in their structure. The presence of delay can stem from its intrinsic properties or from the reuse of system outputs as inputs, as well as the inability to synchronize input-output signals. This delay can have a disruptive effect on both the stability and transient characteristics of the system (Zhong, 2006). Time-delay systems can also appear as models with integrators such as pure integrator plus dead time (PIPD), double integrator plus dead time (DIPDT), etc. Systems with integrators are also frequently encountered in practice. The transfer functions of such systems may have one or more poles at the origin of the s-plane. Therefore, this type of system can produce unbounded output versus bounded input. It is difficult to get a good closed-loop response as this will make the system unstable (Kaya and Peker, 2020). For time-delay systems it is very important to account for the exact delay in the control design, which if ignored will often result in poor performance or even instability. However, due to the complexity of the analysis of such systems, it is difficult to get the exact time-delay in the design process. Therefore, approaches such as Padé, Crude, Limit approach, and Maclaurin series expansion have been developed in the literature to convert the  $e^{-sD}$  exponential function to an integer order transfer function during the design stage of the control system. As the degree of these approaches increases, the real-time delay is approached. However, since the order of the system will increase depending on the degree of approximation, it becomes difficult to solve the characteristic equations. The principal purpose of reduced-order modeling of high-order systems is the simplicity of reduced-order controller design. In addition, many analytical analysis methods can be used for analysis and control of the low-order reduced model of the original system (Garg, 2017; Krishnamurthy and Seshadri, 1978; Sikander and Prasad, 2017). Therefore, Model Order Reduction (MOR) techniques have been developed in the literature to convert high-order systems to low-order systems (Chen, Chang, and Han, 1979; Garg, 2017; Gutman, Mannerfelt, and Molander, 1982; Komarasamy, Albhonso, and Gurusamy, 2012; Krishnamurthy and Seshadri, 1978; Parmar, Mukherjee, and Prasad, 2007; Prajapati and Prasad, 2020; Sinha and Pal, 1990).

In the literature, the problem of controlling time-delay systems has been an important issue. Currently, PI and PID controllers are widely utilized in industrial applications owing to their simple design and robust performance. Generally, in practical applications, PI controllers are preferred more because of the measurement noise caused by the effect of the derivative part (Monje, Chen, Vinagre, Xue, and Feliu-Batlle, 2010). Although the PID controller has only three parameters (proportional gain ( $k_p$ )-integral gain ( $k_i$ ) and derivative gain ( $k_d$ )), it is not easy to find appropriate values of  $k_p$ ,  $k_i$  and  $k_d$  without a systematic rule. Many studies have been done, and some methods have been developed to determine the appropriate parameters in these popular controllers. The most basic known parameter adjustment methods can be listed as Ziegler and Nichols (1942), Astrom and Hägglund (1995), Cohen and Coon (1953), and Tyreus and Luyben (1992) (Åström and Hägglund, 1995; Cohen and Coon, 1953; Tyreus and Luyben, 1992; Ziegler and Nichols, 1942). The tuning methods for these controllers can yield diverse responses in various control systems. Important studies are also carried out on obtaining PID tuning formulas for time-delay systems (Bagis and Senberger, 2017; Kaya, 2021; Malwatkar, Sonawane, and Waghmare, 2009; Onat, 2013; Onat, Hamamci, and Obuz, 2012; Ozyetkin, Onat, and Tan, 2018; Özbek, 2018; Özyetkin, Onat, and Tan, 2012; Özyetkin and Toprak, 2016; Pai, Chang, and Huang, 2010; Tan, 2005; Tyreus and Luyben, 1992). Closed-loop stability is the most critical characteristic that a controller must provide among various design criteria. The stability region, which refers to the set of controller parameters that yield a stable closed loop, is a crucial concept in analyzing the PI controller (Dogruer and Tan, 2018; Rahimian and Tavazoei, 2012). Therefore, it is crucial to calculate the controller parameters that ensure closed-loop stability, and several methods have been developed for this purpose. One of these methods is the Stability Boundary Locus (SBL) technique, which is a graphical approach to determining the controller parameters that stabilize a closed-loop system (Tan, 2005; Tan, Kaya, Yeroglu, and Atherton, 2006). A recent

design method for PI control of time-delay systems involves using the stability region's Weighted Geometric Center (WGC), which is obtained from the SBL method (Onat, 2013).

In this study, PI controllers are designed for time-delay systems using different MOR methods. The method presented is summarized as follows: First, the Padé approach is used to convert time-delay systems to integer order systems. The orders of integer order systems are reduced by Routh stability, Stability equation, Differential equation, and Pole clustering methods. The SBL method was used to obtain the PI parameters that stabilize the reduced models. Appropriate PI parameters within the stable region were determined by the WGC method. Closed-loop unit step responses and performance parameters are obtained by applying the designed PI controllers to the original time-delay model. The preliminary version of this paper was published by Irgan and Tan (2022) in ELECO2022 Symposium (Irgan and Tan, 2022).

The paper is organized as follows: Section 1 provides information on time-delay systems, MOR methods, and controller tuning methods. In Section 2, several MOR methods found in the literature are explained. Section 3 mentions the SBL method to determine the PI controller's stable operating region. Section 4 presents the WGC method to obtain the PI parameters. In Section 5, different high-order time-delay transfer functions are taken as an example, and simulation results are presented. In Section 6, the methods are compared and discussed.

## 2. MODEL ORDER REDUCTION METHODS

First and second order systems, which are important in control systems, are used to express many real systems and are easy to mathematically analyze. For this reason, MOR methods are used to convert high-order systems to low-order systems. Various MOR methods available in the literature are pole clustering methods (Garg, 2017; Komarasamy et al., 2012; Prajapati and Prasad, 2020; Sinha and Pal, 1990), routh stability method (Krishnamurthy and Seshadri, 1978), differential equation method (Gutman et al., 1982), stability equation method (Chen et al., 1979) and coefficient matching method, etc. In this section, the MOR methods available in the literature and used in this study are presented.

### 2.1. Routh Stability Method

This method, developed by Krishnamurthy et al. (1978), is based on the Routh stability criterion (Krishnamurthy and Seshadri, 1978). By creating the Routh table of the model to be reduced, the first two rows of the table are written from the original transfer function, and the coefficients of the remaining rows are calculated according to Equation (1):

$$c_{ab} = \frac{(c_{a-2,1} \times c_{a-1,b+1}) - (c_{a-1,1} \times c_{a-2,b+1})}{c_{a-1,1}}, \quad a \geq 3 \ \& \ b \geq 1 \quad (1)$$

$D_k(s)$ , which the  $k^{th}$ -order reduced polynomial of the original  $n^{th}$ -order polynomial, is written according to Equation (2) using the first two rows of the table containing the order to be reduced:

$$D_k(s) = \sum_{\substack{a=0 \\ b=1}}^{\substack{b:b++ \\ a:a+2 \leq k}} c_{n-k+1,b} s^{k-a} + \sum_{\substack{a=0 \\ b=1}}^{\substack{b:b++ \\ a:a+2 \leq k-1}} c_{n-k+2,b} s^{k-1-a} \quad (2)$$

### 2.2. Differential Equation Method

This method relies on the derivative of both the numerator and denominator polynomials (Gutman et al., 1982). After the original polynomial of  $n^{th}$ -order is changed according to Equation (3), it is successively differentiated as in Equation (4) until a model of  $k^{th}$ -order is obtained.

$$d_n(s) = s^n D_n \left( \frac{1}{s} \right) \quad (3)$$

$$d_k(s) = \frac{\partial^{n-k}}{\partial s^{n-k}} d_n(s) \quad (4)$$

$D_n(s)$  is the original polynomial of  $n^{\text{th}}$ -order,  $d_n(s)$  is the differentiated polynomial, and  $d_k(s)$  is the reduced order differentiated polynomial. The coefficients of the  $d_k(s)$  polynomial are exchanged according to Equation (5) to obtain the normalized reduced order polynomial  $D_k(s)$ .

$$D_k(s) = s^k d_k \left( \frac{1}{s} \right) \quad (5)$$

### 2.3. Stability Equation Method

In this approach developed by Chen T. C. et al. (1979), the reduced model is obtained by decreasing the order of stability equations of the high-order transfer function (Chen et al., 1979).

$$D_n(s) = D_e(s) + D_o(s) \quad (6)$$

Where,  $D_e(s)$  and  $D_o(s)$ , are the even and odd functions of the original polynomial  $D_n(s)$  of  $n^{\text{th}}$ -order, respectively, and are obtained according to Equation (7). These equations are called stability equations. The roots of  $D_e(s)$  and  $D_o(s)$  denote zeros ( $z_i$ ) and poles ( $p_i$ ), respectively.

$$D_e(s) = \sum_{i=0,2,4,\dots}^n b_i s^i = \prod_{i=1}^{n'} (s^2 + z_i^2) \quad (7)$$

$$D_o(s) = \sum_{i=1,3,5,\dots}^n b_i s^i = s \prod_{i=1}^{n'} (s^2 + p_i^2)$$

$n' = n/2$  (if  $n$  is even),  $n' = (n-1)/2$  (if  $n$  is odd). To reduce the stability equations order's, non-dominant zeros/poles are discarded, and the reduced stability equations coefficients are multiplied by the value of the discarded zeros/poles ( $z_D/p_D$ ) as in Equation (8). In this way, the steady-state response of reduced order model remains equivalent to that of the original system.

$$D'_e(s) = z_D^2 \prod_{i=1}^{n'-1} (s^2 + z_{Di}^2) \quad (8)$$

$$D'_o(s) = s \times p_D^2 \prod_{i=1}^{n'-1} (s^2 + p_{Di}^2)$$

Where,  $D'_e(s)$  and  $D'_o(s)$  denote the even and odd functions of the reduced order polynomial, respectively. The reduced stability equations are thus represented by Equation (9):

$$D_{n-1}(s) = D'_e(s) + D_o(s), \quad n \text{ is even} \quad (9)$$

$$D_{n-1}(s) = D_e(s) + D'_o(s), \quad n \text{ is odd}$$

In each zero/pole discarding operation, the order of the model is reduced by 1 order. Accordingly, the zero/pole removal process is continued starting from the highest zero/pole value until the desired lower-order model is obtained.

### 2.4. Pole Clustering Method

Prajapati and Prasad (2020) introduced an enhanced Pole clustering algorithm, which is a variant of the Pole clustering method proposed by Sinha and Pal (1990) (Prajapati and Prasad, 2020). In this method, clusters are created with the original model poles. The number of clusters should be equal to the order of the model to be reduced. An algorithm is used when placing the poles of the original model into the clusters. According to this algorithm, it requires separate clustering for real and complex poles while the system is reduced. Also, the poles on the  $j\omega$ -axis and the origin of the s-plane are kept in the reduced order model. After the poles of the original system in the left half of the s-plane are arranged as  $-p_1, -p_2, \dots, -p_i, \dots, -p_n \forall |p_i| < |p_{i+1}|$ , the cluster centers are determined by placing them in clusters as shown in Equation (10).

$$\begin{aligned}
 c_1 &= - \left\{ \left( \left[ \frac{1}{|p_1|^X} \right] + \left[ \frac{1}{|p_{k+1}|^X} \right] + \left[ \frac{1}{|p_{2k+1}|^X} \right] + \dots + \left[ \frac{1}{|p_{n-k+1}|^X} \right] \right) / a \right\}^{(-1/X)} \\
 c_2 &= - \left\{ \left( \left[ \frac{1}{|p_2|^X} \right] + \left[ \frac{1}{|p_{k+2}|^X} \right] + \left[ \frac{1}{|p_{2k+2}|^X} \right] + \dots + \left[ \frac{1}{|p_{n-k+2}|^X} \right] \right) / b \right\}^{(-1/X)} \\
 &\dots \\
 c_k &= - \left\{ \left( \left[ \frac{1}{|p_k|^X} \right] + \left[ \frac{1}{|p_{2k}|^X} \right] + \left[ \frac{1}{|p_{3k}|^X} \right] + \dots + \left[ \frac{1}{|p_n|^X} \right] \right) / c \right\}^{(-1/X)}
 \end{aligned} \tag{10}$$

Where,  $c_1, c_2, \dots, c_k$  and  $a, b, \dots, c$  denotes the cluster centers and number of poles in these clusters, respectively. The value of  $X$  can be any natural number selected depending on the accuracy required in the reduced order model. If the value of  $X$  is greater than 1, it means that the cluster center is closer to the dominant pole of that cluster. After calculating the cluster centers, the polynomial of the  $k^{th}$ -order reduced order model is obtained as in Equation (11):

$$D_k(s) = (s - c_1)(s - c_2) \dots (s - c_k) \tag{11}$$

### 3. SBL ANALYSIS TO DETERMINE PI CONTROLLERS

The calculation of the controller parameters that stabilize the closed-loop system in control systems is an important issue, and many methods have been developed in the literature for this. SBL analysis, one of these methods, depends on the controller parameters ( $k_p, k_i$ ) and frequency ( $\omega$ ). Since  $\omega$  can vary from 0 to  $\infty$ , it can be calculated with the help of the following equations (Özyetkin and Toprak, 2016; Tan, 2005; Tan et al., 2006). The system transfer function to be controlled in the control system in Figure 1 is given in Equation (12), and the PI controller transfer function is given in Equation (13). The closed-loop characteristic equation of the system  $\Delta(s)$  is obtained as in Equation (14):

$$G(s) = \frac{N(s)}{D(s)} \tag{12}$$

$$C(s) = k_p + \frac{k_i}{s} = \frac{k_p s + k_i}{s} \tag{13}$$

$$\Delta(s) = 1 + C(s)G(s) = (k_p s + k_i)N(s) + sD(s) \tag{14}$$

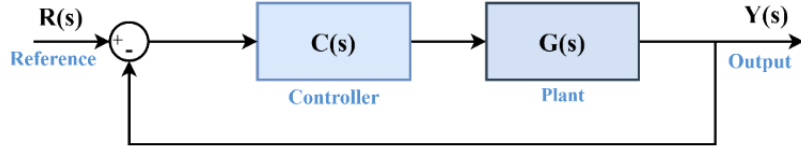


**Figure 1:**  
Feedback control system block diagram.

Equation (15) is formed by separating the numerator and denominator equations of  $G(s)$  into even and odd functions and writing  $s=j\omega$ :

$$G(j\omega) = \frac{N_e(-\omega^2) + j\omega N_o(-\omega^2)}{D_e(-\omega^2) + j\omega D_o(-\omega^2)} \quad (15)$$

Then, the characteristic equation is written as in Equation (16) and Equation (17):

$$\Delta(j\omega) = \left[ k_i N_e(-\omega^2) - k_p \omega^2 N_o(-\omega^2) - \omega^2 D_o(-\omega^2) \right] + j \left[ k_p \omega N_e(-\omega^2) + k_i \omega N_o(-\omega^2) + \omega D_e(-\omega^2) \right] \quad (16)$$

$$\Delta(j\omega) = R_\Delta + jI_\Delta \quad (17)$$

Equation (18) is obtained by equating the real and imaginary parts of  $\Delta(j\omega)$  to zero.

$$\begin{aligned} k_i N_e(-\omega^2) - k_p \omega^2 N_o(-\omega^2) &= \omega^2 D_o(-\omega^2) \\ k_p \omega N_e(-\omega^2) + k_i \omega N_o(-\omega^2) &= -\omega D_e(-\omega^2) \end{aligned} \quad (18)$$

Equations (19)-(20) are obtained by subtracting the unknowns  $k_p$  and  $k_i$  from Equation (18).

$$k_p = \frac{\omega^2 D_o(-\omega^2) N_o(-\omega^2) + D_e(-\omega^2) N_e(-\omega^2)}{-\left( \omega^2 N_o^2(-\omega^2) + N_e^2(-\omega^2) \right)} \quad (19)$$

$$k_i = \frac{\omega^2 D_e(-\omega^2) N_o(-\omega^2) - \omega^2 D_o(-\omega^2) N_e(-\omega^2)}{-\left( \omega^2 N_o^2(-\omega^2) + N_e^2(-\omega^2) \right)} \quad (20)$$

Equations (19) and (20) are solved simultaneously to plot the SBL,  $l(k_p, k_i, \omega)$ , on the  $(k_p-k_i)$  parameter plane in Figure 2. The SBL and  $k_i(0)=0$  real root boundary line divides the  $(k_p-k_i)$  plane to stable and unstable regions (Tan et al., 2006). Since the real root of  $\Delta(s)$  in Equation (14) can pass through the imaginary axis at  $s=0$ , so for  $\omega=0$ ,  $I_\Delta=0$  and  $R_\Delta=0$ ,  $k_i=0$  can be found (Onat et al., 2012; Tan et al., 2006). The SBL graph is drawn on the  $(k_p, k_i)$  plane by solving the  $k_p(\omega)-k_i(\omega)$  equations for each  $\omega$  value for  $\omega \in [0, \omega_{max}]$ . This  $\omega_{max}$  value is the  $\omega$  value that satisfies the equation  $k_i(\omega) = k_i(0) = 0$ . Accordingly, it can be seen from Figure 2 that the  $(k_p, k_i)$  coordinate points are in different positions for each  $\omega$  value. While the points are close to each other at small  $\omega$  values, they are far away at large  $\omega$  values, and when the  $\omega$  value increases too much, the points are very far away from each other. These points end at the real root boundary ( $k_i=0$ ). Here, the number of coordinate points obtained increases and decreases with the step interval of  $\omega$  ( $\Delta\omega$ ). As  $\Delta\omega$  decreases, the number of samples will increase and therefore the controller parameters will be calculated more accurately.

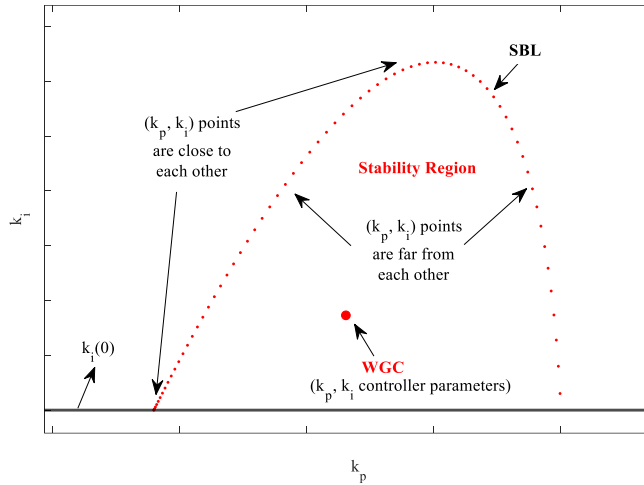


**Figure 2:**  
SBL graph and representation of WGC.

#### 4. CALCULATION OF PI CONTROLLER PARAMETERS WITH WGC METHOD

The WGC method provides the suitable coordinate point(s) within the stability region according to the controller parameters. Since the method is simple to implement, it is a good approach to obtain the suitable operating point. The WGC is calculated using the points from the SBL. This curve covering the stability region is as shown in Figure 2. It consists of  $n$  points with coordinates  $(k_{p1}, k_{i1}), (k_{p2}, k_{i2}), \dots, (k_{pn}, k_{in})$  and  $(k_{p1}, 0), (k_{p2}, 0), \dots, (k_{pn}, 0)$ . Accordingly, the  $k_p$  and  $k_i$  coordinate values of the WGC are calculated using Equation (21) and (22), respectively (Onat, 2013).

$$k_p = \frac{1}{n} \sum_{m=1}^n k_{pm} \tag{21}$$

$$k_i = \frac{1}{2n} \sum_{m=1}^n (k_{im} + k_i(0)) = \frac{1}{2n} \sum_{m=1}^n k_{im} \tag{22}$$

#### 5. SIMULATION STUDIES

In this section, 4<sup>th</sup>-order with low time-delay, high time-delay, and integrating plus time-delay models are examined, respectively. The time-delay terms of the higher order models were first transformed into integer-order models with the Padé approach, and then their orders were reduced with the MOR methods mentioned in the article. Using the block diagram in Figure 1, SBL analysis was performed for the reduced order models, respectively, and appropriate controller parameters within the stable region under these SBL graphs were determined by the WGC method. Accordingly, PI controllers were designed, and the performance of these PI controllers in controlling the original time-delay models was examined.

##### 5.1. Example 1

The 4<sup>th</sup>-order transfer function with 0.1s time-delay given in Equation (23) has been selected from the literature (Malwatkar et al., 2009).

$$G_1(s) = \frac{1}{(s^2 + s + 1)(s + 2)^2} e^{-0.1s} \quad (23)$$

The 6<sup>th</sup>-order integer order transfer function obtained when the 0.1s time-delay in this system is converted to its integer order equivalent with the 2<sup>nd</sup>-order Padé is given in Equation (24).

$$G_{1\text{pade}}(s) = \frac{s^2 - 60s + 1200}{s^6 + 65s^5 + 1509s^4 + 6548s^3 + 11284s^2 + 9840s + 4800} \quad (24)$$

Using the methods introduced in Section 2, the 4<sup>th</sup>-order reduced order transfer functions of the 6<sup>th</sup>-order  $G_{1\text{pade}}(s)$  transfer function are obtained as in Equation (25)- Equation (28).

Differential equation method (Gutman et al., 1982):

$$G_{11}(s) = \frac{30(s^2 - 60s + 1200)}{3018s^4 + 39288s^3 + 135408s^2 + 196800s + 144000} \quad (25)$$

Routh stability method (Krishnamurthy and Seshadri, 1978):

$$G_{12}(s) = \frac{s^2 - 60s + 1200}{1408.26s^4 + 6084.16s^3 + 11132.65s^2 + 9618.45s + 4800} \quad (26)$$

Stability equation method (Chen et al., 1979):

$$G_{13}(s) = \frac{s^2 - 60s + 1200}{1502s^4 + 6449s^3 + 11280s^2 + 9841s + 4800} \quad (27)$$

Pole clustering method (Prajapati and Prasad, 2020) (for  $X=10$ ):

$$G_{14}(s) = \frac{0.9568(s^2 - 60s + 1200)}{1000s^4 + 5072s^3 + 9435s^2 + 8880s + 4593} \quad (28)$$

The unit step responses of the original  $G_1(s)$  model and reduced order  $G_{11}(s)$ ,  $G_{12}(s)$ ,  $G_{13}(s)$ , and  $G_{14}(s)$  models are shown in Figure 3. When the unit step responses in Figure 3 are examined, it is concluded that the reduced order models obtained by all methods converge quite well to the original model ( $G_1(s)$ ). Although it is seen that the model obtained by the Differential equation method ( $G_{11}(s)$ ) converges less to the original model than the other models, the  $G_{12}(s)$ ,  $G_{13}(s)$ , and  $G_{14}(s)$  models obtained by the Routh stability, Stability equation and Pole clustering methods converge almost exactly to the original model, respectively.

SBL analysis was performed for the reduced order  $G_{11}(s)$ ,  $G_{12}(s)$ ,  $G_{13}(s)$ , and  $G_{14}(s)$  models and the  $k_p$  and  $k_i$  equations related to  $\omega$  were obtained as in Equation (29)- Equation (36).

For  $G_{11}(s)$  model;

$$k_p = \frac{8.149e07\omega^{10} - 6.542e11\omega^8 + 8.836e14\omega^6 - 2.648e17\omega^4 + 6.81e18\omega^2 - 6.718e18}{810000\omega^8 - 3.89e09\omega^6 + 7.002e12\omega^4 - 5.601e15\omega^2 + 1.68e18} \quad (29)$$

$$k_i = \frac{6.611e06\omega^6 - 1.664e09\omega^4 + 7.344e09\omega^2}{900\omega^4 + 1.08e06\omega^2 + 1.296e09} \quad (30)$$

For  $G_{12}(s)$  model;

$$k_p = \frac{1408\omega^{10} - 1.06e07\omega^8 + 1.322e10\omega^6 - 3.057e12\omega^4 + 2.011e13\omega^2 - 8.294e12}{\omega^8 - 4860\omega^6 + 8.784e06\omega^4 - 6.998e09\omega^2 + 2.074e12} \quad (31)$$

$$k_i = \frac{90564\omega^6 - 7.978e06\omega^4 + 1.183e07\omega^2}{\omega^4 + 1200\omega^2 + 1.44e06} \quad (32)$$

For  $G_{13}(s)$  model;

$$k_p = \frac{1502\omega^{10} - 1.13e07\omega^8 + 1.41e10\omega^6 - 3.252e12\omega^4 + 2.038e13\omega^2 - 8.294e12}{\omega^8 - 4860\omega^6 + 8.784e06\omega^4 - 6.998e09\omega^2 + 2.074e12} \quad (33)$$

$$k_i = \frac{96569\omega^6 - 8.425e06\omega^4 + 1.21e07\omega^2}{\omega^4 + 1200\omega^2 + 1.44e06} \quad (34)$$

For  $G_{14}(s)$  model;

$$k_p = \frac{8.759e-10\omega^{10} - 6.151e-05\omega^8 + 0.0747\omega^6 - 2.592\omega^4 + 15.29\omega^2 - 6.952}{8.381e-13\omega^8 - 5.658e-08\omega^6 + 0.0001334\omega^4 - 0.08147\omega^2 + 1.738} \quad (35)$$

$$k_i = \frac{0.06226\omega^6 - 6.374\omega^4 + 10.46\omega^2}{9.155e-07\omega^4 + 0.001099\omega^2 + 1.318} \quad (36)$$

For the  $G_{11}(s)$ ,  $G_{12}(s)$ ,  $G_{13}(s)$ , and  $G_{14}(s)$  models, the appropriate  $k_p$  and  $k_i$  values were obtained with the help of the WGC equations given in (21) and (22). Accordingly, SBL graphs and WGC points were obtained for the  $G_{11}(s)$ ,  $G_{12}(s)$ ,  $G_{13}(s)$ , and  $G_{14}(s)$  models, respectively, as in Figure 4. The  $\omega$  values satisfying the  $k_i=0$  equation in the SBL graphs of the  $G_{11}(s)$ ,  $G_{12}(s)$ ,  $G_{13}(s)$ , and  $G_{14}(s)$  models in Figure 4 were found to be 2.1198, 1.2282, 1.2084 and 1.2916, respectively. After obtaining the appropriate  $k_p$  and  $k_i$  values in the stability region with the WGC method as in Figure 4,  $G_{c1}(s)$ ,  $G_{c2}(s)$ ,  $G_{c3}(s)$ , and  $G_{c4}(s)$  PI controllers were designed, respectively, and these PI controllers were applied to the original  $G_1(s)$  model.

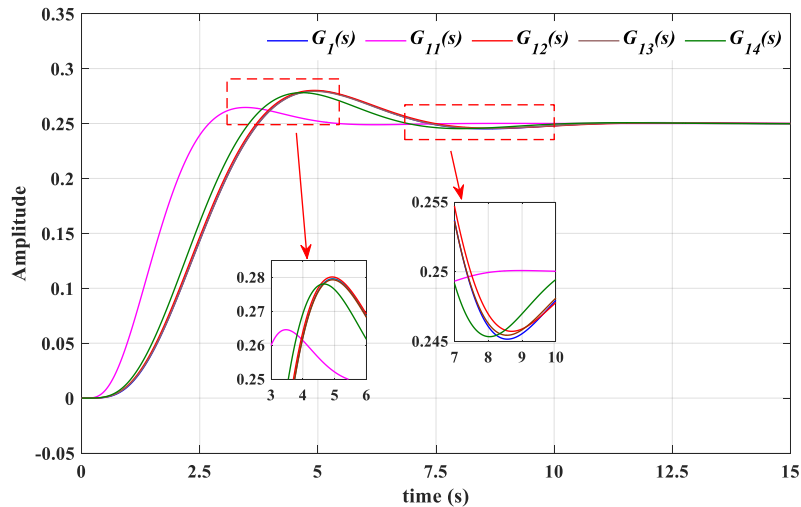


**Figure 3:** Unit step responses of original  $G_1(s)$  model and reduced  $G_{11}(s)$ ,  $G_{12}(s)$ ,  $G_{13}(s)$ ,  $G_{14}(s)$  models.

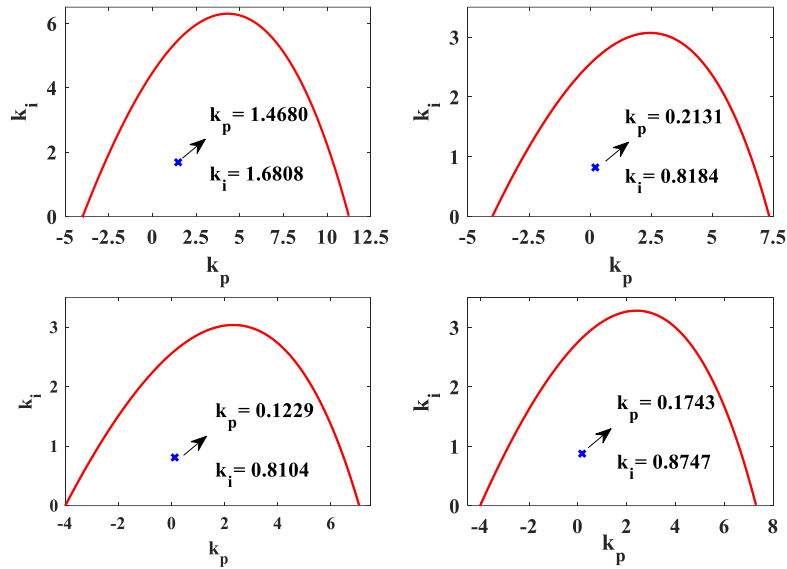


**Figure 4:**  
SBL graphs for reduced order models  $G_{11}(s)$ ,  $G_{12}(s)$ ,  $G_{13}(s)$ , and  $G_{14}(s)$ .

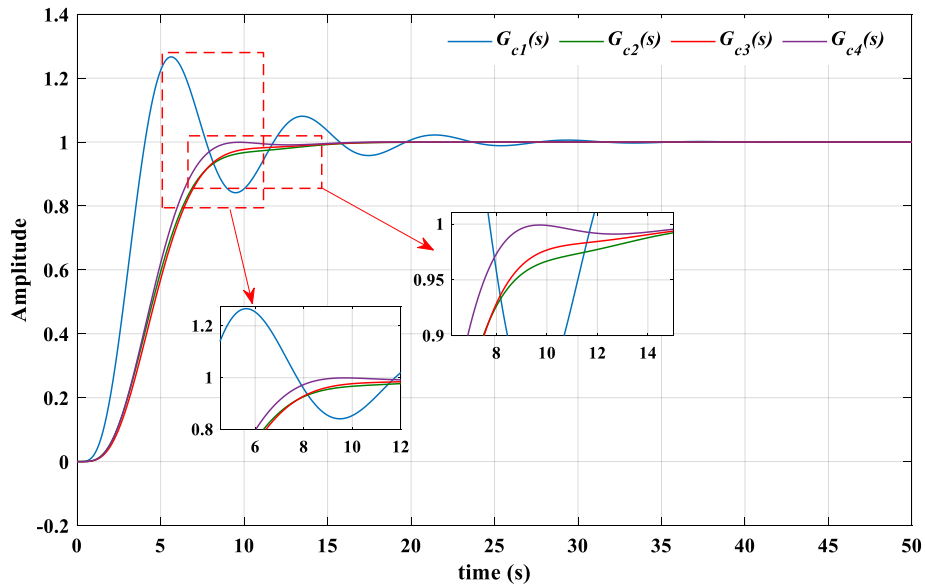


**Figure 5:**  
Closed-loop step responses for  $G_1(s)$  model.

The closed-loop unit step responses obtained are shown in Figure 5 and the performance values are shown in Table 1. When the closed-loop unit step responses in Figure 5 and the performance values in Table 1 are examined, it is seen that the  $G_{c1}(s)$  controller designed according to the  $G_{11}(s)$  model obtained by the Differential equation method controls the original  $G_1(s)$  system worse than the other controllers. However, it is seen that  $G_{c2}(s)$ ,  $G_{c3}(s)$ , and  $G_{c4}(s)$  controllers designed using  $G_{12}(s)$ ,  $G_{13}(s)$ , and  $G_{14}(s)$  models obtained by Routh stability, Stability equation, and Pole clustering methods control the original  $G_1(s)$  system with good performance.

According to these values, it is concluded that Routh stability, Stability equation and Pole clustering MOR methods can be used effectively while designing the controller in short time-delay systems.

## 5.2. Example 2

The 4<sup>th</sup>-order transfer function with 3s time-delay given in Equation (37) has been selected from the literature (Huang, Jeng, and Luo, 2005).

$$G_2(s) = \frac{1}{(s^2 + 10s + 1)(s + 1)^2} e^{-3s} \quad (37)$$

The 6<sup>th</sup>-order integer order transfer function obtained when the 3s time-delay in this system is converted to its integer order equivalent with the 2<sup>nd</sup>-order Padé is given in Equation (38).

$$G_{2\text{pade}}(s) = \frac{s^2 - 2s + 1.333}{s^6 + 14s^5 + 47.33s^4 + 72s^3 + 54.33s^2 + 18s + 1.333} \quad (38)$$

Using the methods introduced in Section 2, the 4<sup>th</sup>-order reduced order transfer functions of the 6<sup>th</sup>-order  $G_{2\text{pade}}(s)$  transfer function are obtained as in Equation (39)- Equation (42):

Differential equation method (Gutman et al., 1982):

$$G_{21}(s) = \frac{30(s^2 - 2s + 1.333)}{94.66s^4 + 432s^3 + 652s^2 + 360s + 39.99} \quad (39)$$

Routh stability method (Krishnamurthy and Seshadri, 1978):

$$G_{22}(s) = \frac{s^2 - 2s + 1.333}{42.19s^4 + 54.4s^3 + 53.04s^2 + 17.56s + 1.333} \quad (40)$$

Stability equation method (Chen et al., 1979):

$$G_{23}(s) = \frac{s^2 - 2s + 1.333}{46.15s^4 + 68.31s^3 + 54.31s^2 + 18s + 1.333} \quad (41)$$

Pole clustering method (Prajapati and Prasad, 2020) (for  $X=10$ ):

$$G_{24}(s) = \frac{0.1052(s^2 - 2s + 1.333)}{s^4 + 3.142s^3 + 3.723s^2 + 1.733s + 0.1402} \quad (42)$$

The unit step responses of the original  $G_2(s)$  model and reduced order  $G_{21}(s)$ ,  $G_{22}(s)$ ,  $G_{23}(s)$ , and  $G_{24}(s)$  models are shown in Figure 6. When the unit step responses in Figure 6 are examined, it is concluded that the reduced order models obtained by all methods converge to the original model ( $G_2(s)$ ). Although it is seen that the model obtained by the Differential equation method ( $G_{21}(s)$ ) converges less than the other models, the  $G_{22}(s)$  and  $G_{23}(s)$  models obtained by the Routh stability and Stability equation methods, respectively, converge to the original model more. In addition, the convergence of the reduced  $G_{24}$  model obtained by the Pole clustering method to the original model is less than in Example 1. This is because high value poles move the cluster center away from the dominant poles. This reduces the convergence to the original model. Moreover, the integer equivalent model obtained with the 2<sup>nd</sup>-order Padé approach has an inverse response. Thus, the reduced order models converge less to the original model.

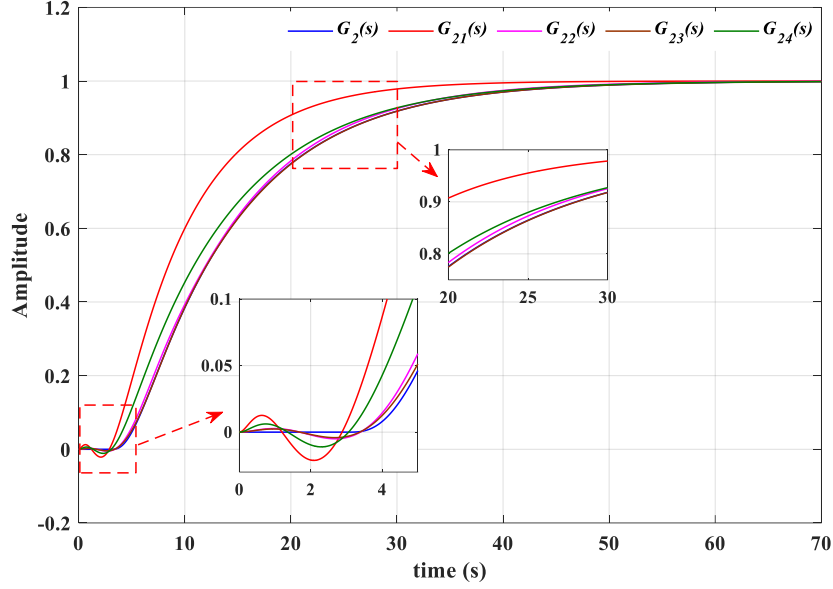


**Figure 6:**

Unit step responses of original  $G_2(s)$  model and reduced  $G_{21}(s)$ ,  $G_{22}(s)$ ,  $G_{23}(s)$ ,  $G_{24}(s)$  models.

SBL analysis was performed for the reduced order  $G_{21}(s)$ ,  $G_{22}(s)$ ,  $G_{23}(s)$ , and  $G_{24}(s)$  models and the  $k_p$  and  $k_i$  equations related to  $\omega$  were obtained as in Equation (43)- Equation (50).

For  $G_{21}(s)$  model;

$$k_p = \frac{2.556e06\omega^{10} - 6.155e07\omega^8 + 2.522e08\omega^6 - 2.973e08\omega^4 + 8.785e07\omega^2 - 2.557e06}{810000\omega^8 - 4.373e06\omega^6 + 8.78e06\omega^4 - 7.77e06\omega^2 + 2.557e06} \quad (43)$$

$$k_i = \frac{1.864e04\omega^6 - 1.864e04\omega^4 + 1.68e04\omega^2}{900\omega^4 + 1201\omega^2 + 1599} \quad (44)$$

For  $G_{22}(s)$  model;

$$k_p = \frac{42.19\omega^{10} - 583.7\omega^8 + 1419\omega^6 - 1107\omega^4 + 205.8\omega^2 - 3.157}{\omega^8 - 7.332\omega^6 + 15.99\omega^4 - 13.03\omega^2 + 3.157} \quad (45)$$

$$k_i = \frac{138.8\omega^6 - 196.2\omega^4 + 26.07\omega^2}{\omega^4 + 1.334\omega^2 + 1.777} \quad (46)$$

For  $G_{23}(s)$  model;

$$k_p = \frac{46.15\omega^{10} - 652.4\omega^8 + 1560\omega^6 - 1185\omega^4 + 210.4\omega^2 - 3.157}{\omega^8 - 7.332\omega^6 + 15.99\omega^4 - 13.03\omega^2 + 3.157} \quad (47)$$

$$k_i = \frac{160.6\omega^6 - 217.7\omega^4 + 26.66\omega^2}{\omega^4 + 1.334\omega^2 + 1.777} \quad (48)$$

For  $G_{24}(s)$  model;

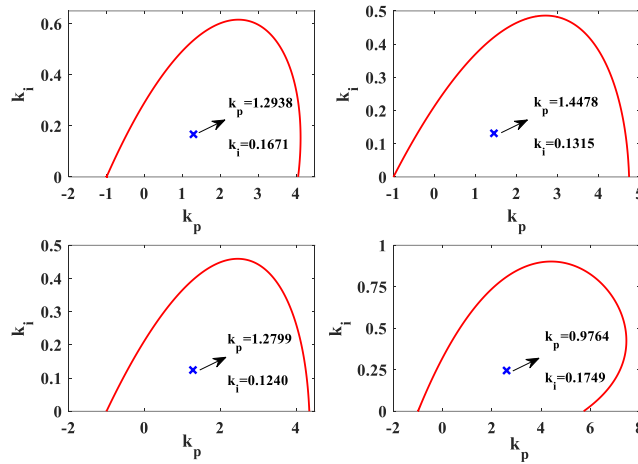


**Figure 7:**  
SBL graphs for reduced order models  $G_{21}(s)$ ,  $G_{22}(s)$ ,  $G_{23}(s)$ , and  $G_{24}(s)$ .

$$k_p = \frac{\omega^{10} - 56.33\omega^8 + 332.6\omega^6 - 437.7\omega^4 + 125.1\omega^2 - 3.157}{\omega^8 - 7.332\omega^6 + 15.99\omega^4 - 13.03\omega^2 + 3.157} \tag{49}$$

$$k_i = \frac{14\omega^6 - 75.99\omega^4 + 23.1\omega^2}{\omega^4 + 1.334\omega^2 + 1.777} \tag{50}$$

After obtaining the  $k_p$  and  $k_i$  equations for the  $G_{21}(s)$ ,  $G_{22}(s)$ ,  $G_{23}(s)$ , and  $G_{24}(s)$  models, the appropriate  $k_p$  and  $k_i$  values were obtained with the help of the WGC equations in Equation (21) and (22). Accordingly, SBL graphs and WGC points were obtained for the  $G_{21}(s)$ ,  $G_{22}(s)$ ,  $G_{23}(s)$ , and  $G_{24}(s)$  models, respectively, as in Figure 7. In the SBL graphs of the  $G_{21}(s)$ ,  $G_{22}(s)$ ,  $G_{23}(s)$ , and  $G_{24}(s)$  models in Figure 7, the  $\omega$  values satisfying the  $k_i=0$  equations were found to be 0.5198, 0.3854, 0.3690, and 0.4592, respectively.

The appropriate  $k_p$  and  $k_i$  values in the stability region were obtained using the WGC method for the  $G_{21}(s)$ ,  $G_{22}(s)$ ,  $G_{23}(s)$ , and  $G_{24}(s)$  models as shown in Figure 7. Then, PI controllers  $G_{c1}(s)$ ,  $G_{c2}(s)$ ,  $G_{c3}(s)$ , and  $G_{c4}(s)$  were designed, respectively, and these PI controllers were applied to the original  $G_2(s)$  model. The closed-loop unit step responses obtained are shown in Figure 8 and the performance values are shown in Table 1.

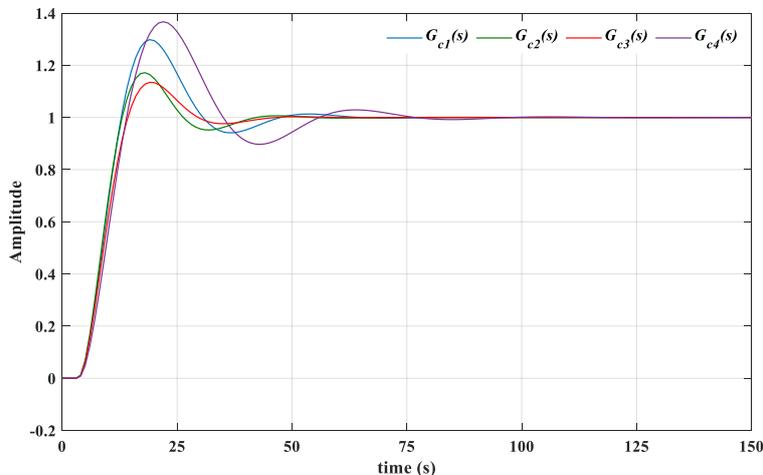


**Figure 8:**  
Closed-loop step responses for  $G_2(s)$  model.

When the closed-loop unit step responses in Figure 8 and the performance values in Table 1 are examined, it is concluded that the  $G_{c4}(s)$  controller designed according to the  $G_{24}(s)$  model obtained by the Pole clustering method controls the original  $G_2(s)$  system worse than the other controllers. It is seen that the  $G_{c2}(s)$  and  $G_{c3}(s)$  controllers designed using the  $G_{22}(s)$  and  $G_{23}(s)$  models obtained by Routh stability and Stability equation methods control the original  $G_2(s)$  system with good performance. According to these values, it is concluded that the Routh stability and Stability equation MOR methods can be used more effectively than other methods when designing the controller in long time-delay systems.

### 5.3. Example 3

The 4<sup>th</sup>-order integrating transfer function with 2s time-delay given in Equation (51) has been selected from the literature (Peker and Kaya, 2022).

$$G_3(s) = \frac{1}{s(s+1)(0.5s+1)(0.25s+1)} e^{-2s} \quad (51)$$

The 6<sup>th</sup>-order integer order transfer function obtained when the 2s time-delay in this system is converted to its integer order equivalent with the 2<sup>nd</sup>-order Padé is given in Equation (52).

$$G_{3pade}(s) = \frac{s^2 - 3s + 3}{0.125s^6 + 1.25s^5 + 4.75s^4 + 8.875s^3 + 8.25s^2 + 3s} \quad (52)$$

Using the methods introduced in Section 2, the 4<sup>th</sup>-order reduced order transfer functions of the 6<sup>th</sup>-order  $G_{3pade}(s)$  transfer function are obtained as in Equation (53)- Equation (56).

Differential equation method (Gutman et al., 1982):

$$G_{31}(s) = \frac{20(s^2 - 3s + 3)}{9.5s^4 + 53.25s^3 + 99s^2 + 60s} \quad (53)$$

Routh stability method (Krishnamurthy and Seshadri, 1978):

$$G_{32}(s) = \frac{s^2 - 3s + 3}{3.862s^4 + 6.302s^3 + 7.95s^2 + 3s} \quad (54)$$

Stability equation method (Chen et al., 1979):

$$G_{33}(s) = \frac{s^2 - 3s + 3}{4.522s^4 + 8.43s^3 + 8.25s^2 + 2.999s} \quad (55)$$

Pole clustering method (Prajapati and Prasad, 2020) (for  $X=10$ ):

$$G_{34}(s) = \frac{1.116(s^2 - 3s + 3)}{s^4 + 4.116s^3 + 6.348s^2 + 3.348s} \quad (56)$$

The unit step responses of the original  $G_3(s)$  model and reduced order  $G_{31}(s)$ ,  $G_{32}(s)$ ,  $G_{33}(s)$ , and  $G_{34}(s)$  models are shown in Figure 9.

When the unit step responses in Figure 9 are examined, it is concluded that the reduced order models obtained by all methods converge to the original model ( $G_3(s)$ ) quite a lot. It is seen that the models ( $G_{31}(s)$  and  $G_{34}(s)$ ) obtained by Differential equation and Pole clustering methods converge less to the original model than other models. The  $G_{32}(s)$  and  $G_{33}(s)$  models, obtained by the Routh stability and Stability equation, respectively, converge almost exactly to the original model. In addition, unstable zeros occur in the integer order equivalent model obtained with Padé. This causes an inverse response in the reduced models. SBL analysis was performed for the reduced order models  $G_{31}(s)$ ,  $G_{32}(s)$ ,  $G_{33}(s)$ , and  $G_{34}(s)$  and the  $k_p$  and  $k_i$  equations related to  $\omega$  were obtained as in Equation (57)- Equation (64).

For  $G_{31}(s)$  model;

$$k_p = \frac{76000\omega^{10} - 3.449e06\omega^8 + 2.762e07\omega^6 - 6.532e07\omega^4 + 3.434e07\omega^2}{160000\omega^8 - 1.944e06\omega^6 + 8.784e06\omega^4 - 1.75e07\omega^2 + 1.296e07} \quad (57)$$

$$k_i = \frac{1635\omega^6 - 10335\omega^4 + 3600\omega^2}{400\omega^4 + 1200\omega^2 + 3600} \quad (58)$$

For  $G_{32}(s)$  model;

$$k_p = \frac{3.862\omega^{10} - 108\omega^8 + 532.7\omega^6 - 829.3\omega^4 + 295.6\omega^2}{\omega^8 - 15\omega^6 + 72\omega^4 - 135\omega^2 + 81} \quad (59)$$

$$k_i = \frac{17.89\omega^6 - 45.76\omega^4 + 9\omega^2}{\omega^4 + 3\omega^2 + 9} \quad (60)$$

For  $G_{33}(s)$  model;

$$k_p = \frac{4.522\omega^{10} - 128.5\omega^8 + 618.9\omega^6 - 923.4\omega^4 + 303.7\omega^2}{\omega^8 - 15\omega^6 + 72\omega^4 - 135\omega^2 + 81} \quad (61)$$

$$k_i = \frac{22\omega^6 - 53.4\omega^4 + 8.997\omega^2}{\omega^4 + 3\omega^2 + 9} \quad (62)$$

For  $G_{34}(s)$  model;

$$k_p = \frac{1.39\omega^{10} - 54.74\omega^8 + 385.7\omega^6 - 823.4\omega^4 + 363.9\omega^2}{1.551\omega^8 - 22.78\omega^6 + 108.8\omega^4 - 205.1\omega^2 + 125.6} \quad (63)$$

$$k_i = \frac{7.941\omega^6 - 38.77\omega^4 + 11.21\omega^2}{1.245\omega^4 + 3.736\omega^2 + 11.21} \quad (64)$$

For the  $G_{31}(s)$ ,  $G_{32}(s)$ ,  $G_{33}(s)$ , and  $G_{34}(s)$  models, after obtaining the  $k_p$  and  $k_i$  equations related to  $\omega$ , the appropriate  $k_p$  and  $k_i$  values were obtained with the help of the WGC equations given in (21) and (22). Accordingly, SBL graphs and WGC points were obtained for the  $G_{31}(s)$ ,  $G_{32}(s)$ ,  $G_{33}(s)$ , and  $G_{34}(s)$  models, respectively, as in Figure 10. In the SBL graphs of the  $G_{31}(s)$ ,  $G_{32}(s)$ ,  $G_{33}(s)$ , and  $G_{34}(s)$  models in Figure 10, the  $\omega$  values satisfying the  $k_i=0$  equations were found to be 0.6083, 0.4634, 0.4285, and 0.5555, respectively.

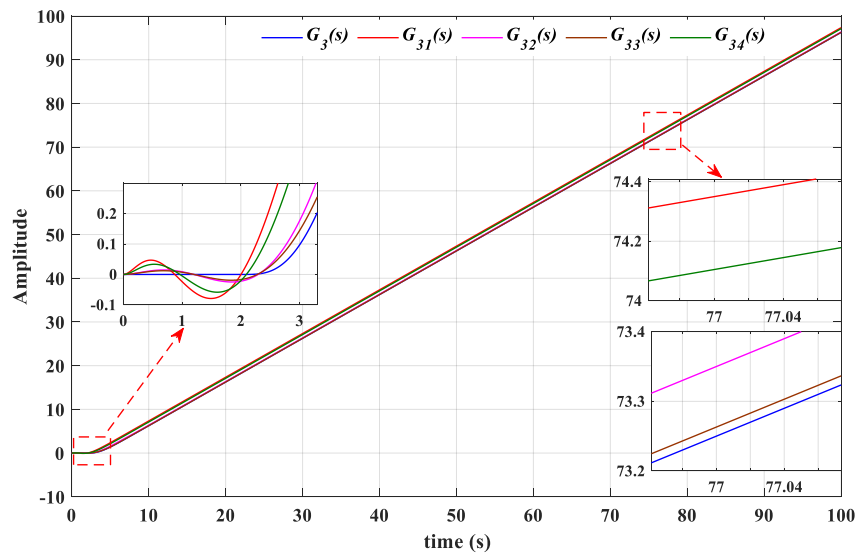


**Figure 9:**

Unit step responses of original  $G_3(s)$  model and reduced  $G_{31}(s)$ ,  $G_{32}(s)$ ,  $G_{33}(s)$ ,  $G_{34}(s)$  models.

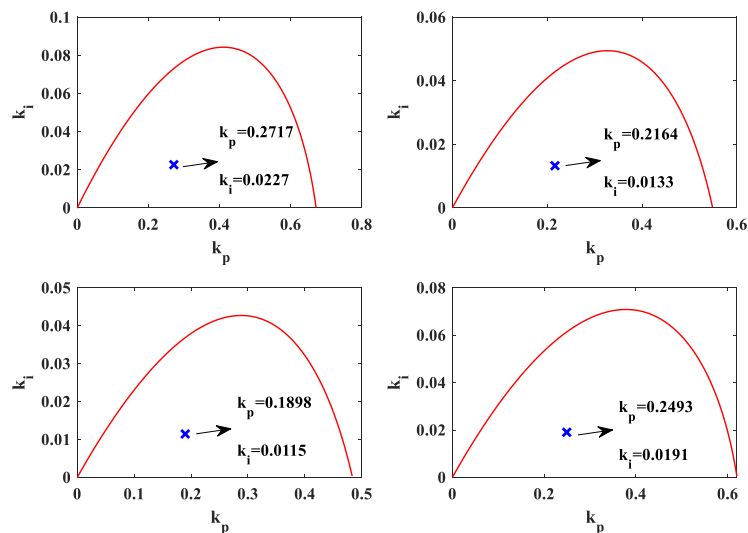


**Figure 10:**

SBL graphs for reduced order models  $G_{31}(s)$ ,  $G_{32}(s)$ ,  $G_{33}(s)$ , and  $G_{34}(s)$ .

After obtaining the appropriate  $k_p$  and  $k_i$  values in the stability region with the WGC method for the  $G_{31}(s)$ ,  $G_{32}(s)$ ,  $G_{33}(s)$ , and  $G_{34}(s)$  models as in Figure 10,  $G_{c1}(s)$ ,  $G_{c2}(s)$ ,  $G_{c3}(s)$ , and  $G_{c4}(s)$  PI controllers were designed, and these PI controllers were applied to the original  $G_3(s)$  model. The closed-loop unit step responses obtained are shown in Figure 11 and performance values are shown in Table 1. When the closed-loop unit step responses in Figure 11 and the performance values in Table 1 are examined, it is concluded that the  $G_{c1}(s)$  and  $G_{c4}(s)$  controllers designed according to the  $G_{31}(s)$  and  $G_{34}(s)$  models obtained by the Differential equation and Pole clustering methods control the original  $G_3(s)$  system worse than the other controllers. However, it is seen that the  $G_{c2}(s)$  and  $G_{c3}(s)$  controllers designed using the  $G_{32}(s)$  and  $G_{33}(s)$  models obtained by the Routh stability and Stability equation methods control the original  $G_3(s)$  system with good performance. According to these values, it is concluded that the Routh stability and Stability equation MOR methods can be used more effectively when designing the controller for long time-delay with integrating systems.

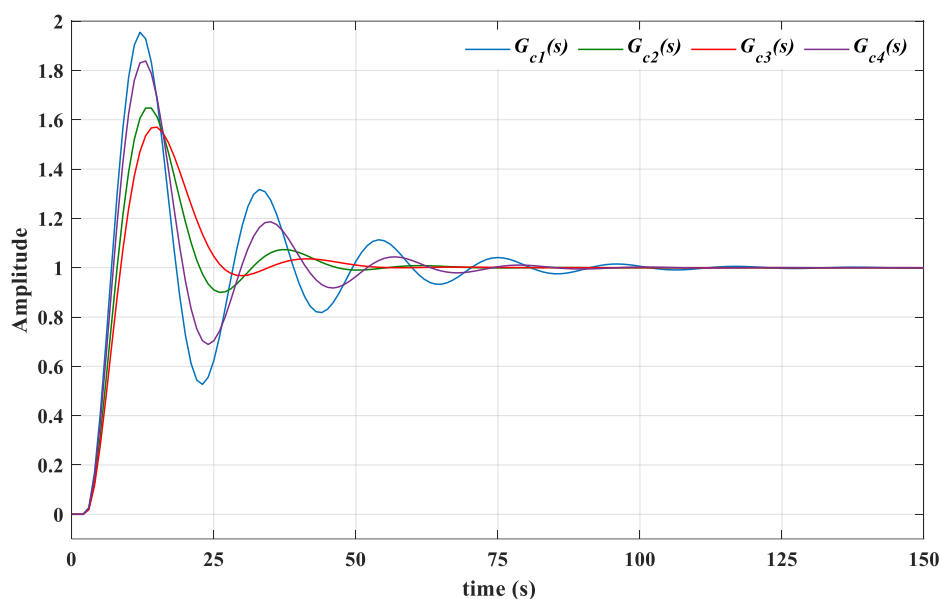


**Figure 11:**  
Closed-loop step responses for  $G_3(s)$  model.

**Table 1. Parameters and performance values of PI controllers designed according to reduced order models for  $G_1(s)$ ,  $G_2(s)$  and  $G_3(s)$  original models.**

<i>Original model</i>	<i>Parameters and performance values</i>	$G_{c1}(s)$	$G_{c2}(s)$	$G_{c3}(s)$	$G_{c4}(s)$
$G_1(s)$	$k_p$	1.4680	0.2131	0.1229	0.1743
	$k_i$	1.6808	0.8184	0.8104	0.8747
	$t_r(s)$	2.2081	5.0091	5.0260	4.4806
	$t_s(s)$	21.9669	12.5325	10.5357	8.1904
	$M_p(\%)$	26.5927	0	0	0
$G_2(s)$	$k_p$	1.2938	1.4478	1.2799	0.9764
	$k_i$	0.1671	0.1315	0.1240	0.1749
	$t_r(s)$	6.4369	6.5425	7.3689	7.2578
	$t_s(s)$	44.1019	38.0751	38.0035	69.4744
	$M_p(\%)$	0.2717	0.2164	0.1898	0.2493
$G_3(s)$	$k_p$	0.0227	0.0133	0.0115	0.0191
	$k_i$	3.0638	3.7608	4.2083	3.2974
	$t_r(s)$	87.6134	44.1682	47.3458	68.7917
	$t_s(s)$	95.5217	65.1760	57.1695	84.2576
	$M_p(\%)$	29.8429	17.1756	13.4963	36.6953

## 6. CONCLUSIONS

In this study, the time-delay models were examined using the Differential equation, Routh stability, Stability equation, and Pole clustering MOR methods available in the literature, and these models were applied using the Padé approach. The unit step responses of the reduced-order models were examined. Accordingly, it is seen that the reduced order models obtained with the Routh stability, Stability equation, and Pole clustering methods converge more to the original model than the reduced order models obtained with the Differential equation method. However, as the time delay value increases, the convergence of the reduced order model obtained with the Pole clustering method to the original model decreases. This is because high value poles move the cluster center away from the dominant poles. This reduces the convergence of the reduced order model to the original time delay model. In addition, the integer order equivalent models obtained by the 2<sup>nd</sup>-order Padé approach have an inverse response due to unstable zeros. Thus, the reduced order models converge less to the original model. An integrating with time delay system is also studied as an example, and unit step responses are examined. In this case, it was seen that the reduced order models obtained by all methods converged quite well to the original model. It is observed that the models obtained by the differential equation and pole clustering methods converge less with the original model than the other models. On the other hand, the models obtained with Routh stability and the Stability equation appear to converge almost exactly to the original model.

Then, SBL analyzes were performed for these reduced-order models, and SBL graphs of the PI controller parameters were obtained. After obtaining the  $k_p$  and  $k_i$  equations depending on  $\omega$  by the SBL method, the appropriate  $k_p$  and  $k_i$  values were obtained by the WGC method, and  $G_{c1}(s)$ - $G_{c4}(s)$  controllers were designed. Closed-loop responses and performance values are obtained by applying these controllers to the original time-delay models. According to these analyzes, it is seen that the controllers designed using the models obtained by the Routh stability, Stability equation, and Pole clustering methods in the short time-delay system control the original time-delay system with good performance. However, it is seen that the controller designed according to the model obtained by the Differential equation method controls the original time-delay system worse than the other controllers. In the case of long dead-time and integrating with long dead-time models, it is seen that the controllers designed using the models obtained with the Routh stability and Stability equation control the original time-delay system with good performance, while the controllers obtained by the Differential equation method and Pole clustering methods control worse.

## CONFLICT OF INTEREST

The authors state that they do not have any known conflicts of interest or shared interests with any institutions/organizations or individuals.

## AUTHOR CONTRIBUTION

Hilal İRGAN and Nusret TAN are both authors of the study. İrgan contributed to the literature review, data collection, data processing and analysis, and writing of the article, while Tan contributed to the determination and management of the study's conceptual and design processes, data analysis and interpretation, and critical review and control of the article. All authors have given their final approval and take full responsibility for the work.

## REFERENCES

1. Åström, K. J. and Hägglund, T. (1995) *PID Controllers: Theory, Design, and Tuning* (2nd ed.), Research Triangle Park, North Carolina: ISA - The Instrumentation, Systems and Automation Society.
2. Bagis, A. and Senberger, H. (2017) ABC algorithm based PID controller design for higher order oscillatory systems, *Elektronika ir Elektrotechnika*, 23(6). doi:10.5755/j01.eie.23.6.19688
3. Chen, T., Chang, C. and Han, K. (1979) Reduction of transfer functions by the stability-equation method, *Journal of the Franklin Institute*, 308(4), 389-404. doi:10.1016/0016-0032(79)90066-8
4. Cohen, G. and Coon, G. (1953) Theoretical consideration of retarded control, *Transactions of the American Society of Mechanical Engineers*, 75(5), 827-834. doi:10.1115/1.4015451
5. Dogruer, T. and Tan, N. (2018) Design of PI controller using optimization method in fractional order control systems, *IFAC-PapersOnLine*, 51(4), 841-846. doi:10.1016/j.ifacol.2018.06.124
6. Garg, M. (2017) *Model order reduction and approximation analysis for control system design*, 4th International Conference on Signal Processing, Computing and Control (ISPCC), Solan, India, doi:10.1109/ISPCC.2017.8269725
7. Gutman, P., Mannerfelt, C. and Molander, P. (1982) Contributions to the model reduction problem, *IEEE Transactions on Automatic Control*, 27(2), 454-455. doi:10.1109/TAC.1982.1102930
8. Huang, H.-P., Jeng, J.-C. and Luo, K.-Y. (2005) Auto-tune system using single-run relay feedback test and model-based controller design, *Journal of process control*, 15(6), 713-727. doi:10.1016/j.jprocont.2004.11.004
9. Irgan, H. and Tan, N. (2022), *Model Derecesi İndirgeme Yöntemleri Kullanılarak Zaman Gecikmeli Sistemlerde Ağırlıklı Geometrik Merkez Yöntemi ile PI Kontrolör Tasarımı* International Conference on Electrical and Electronics Engineering (ELECO), Bursa, Turkey.
10. Kaya, I. (2021) Optimal PI–PD controller design for pure integrating processes with time delay, *Journal of Control, Automation and Electrical Systems*, 32(3), 563-572. doi:10.1007/s40313-021-00692-2
11. Kaya, I. and Peker, F. (2020) Optimal I-PD controller design for setpoint tracking of integrating processes with time delay, *IET Control Theory & Applications*, 14(18), 2814-2824. doi:10.1049/iet-cta.2019.1378
12. Komarasamy, R., Albhonso, N. and Gurusamy, G. (2012) Order reduction of linear systems with an improved pole clustering, *Journal of vibration and control*, 18(12), 1876-1885. doi:10.1177/1077546311426592
13. Krishnamurthy, V. and Seshadri, V. (1978) Model reduction using the Routh stability criterion, *IEEE Transactions on Automatic control*, 23(4), 729-731. doi:10.1109/TAC.1978.1101805
14. Malwatkar, G., Sonawane, S. and Waghmare, L. (2009) Tuning PID controllers for higher-order oscillatory systems with improved performance, *ISA transactions*, 48(3), 347-353. doi:10.1016/j.isatra.2009.04.005
15. Monje, C. A., Chen, Y., Vinagre, B. M., Xue, D. and Feliu-Battle, V. (2010) *Fractional-order systems and controls: fundamentals and applications*: Springer Science & Business Media. doi:10.1007/978-1-84996-335-0
16. Onat, C. (2013) A new concept on PI design for time delay systems: weighted geometrical center, *International Journal of Innovative Computing, information and control*, 9(4), 1539-1556.

17. Onat, C., Hamamci, S. E. and Obuz, S. (2012) A practical PI tuning approach for time delay systems, *IFAC Proceedings Volumes*, 45(14), 102-107. doi:10.3182/20120622-3-US-4021.00027
18. Özyetkin, M., Onat, C. and Tan, N. (2018) PID tuning method for integrating processes having time delay and inverse response, *IFAC-PapersOnLine*, 51(4), 274-279. doi:10.1016/j.ifacol.2018.06.077
19. Özbek, N. (2018). Control of time-delayed systems with experimental applications. *Doctorate thesis*, Çukurova University Graduate School of Natural and Applied Sciences, Adana.
20. Özyetkin, M. M., Onat, C. and Tan, N. (2012) *Zaman Gecikmeli Sistemler için Denetçi Tasarımı*, Otomatik Kontrol Ulusal Toplantısı TOK-2012, Niğde,
21. Özyetkin, M. M. and Toprak, A. (2016) Ağırlıklı geometrik merkez metodu ile pratik PI-PD kontrolör tasarımı, *Dicle Üniversitesi Mühendislik Fakültesi Mühendislik Dergisi*, 7(3), 595-605.
22. Pai, N.-S., Chang, S.-C. and Huang, C.-T. (2010) Tuning PI/PID controllers for integrating processes with deadtime and inverse response by simple calculations, *Journal of process control*, 20(6), 726-733. doi:10.1016/j.jprocont.2010.04.003
23. Parmar, G., Mukherjee, S. and Prasad, R. (2007) Reduced order modelling of linear dynamic systems using particle swarm optimized eigen spectrum analysis, *International Journal of Electrical and Computer Engineering*, 1(1), 73-80. doi:10.5281/zenodo.1083457
24. Peker, F. and Kaya, I. (2022) Maximum sensitivity (Ms)-based I-PD controller design for the control of integrating processes with time delay, *International Journal of Systems Science*, 1-20. doi:10.1080/00207721.2022.2122759
25. Prajapati, A. K. and Prasad, R. (2020) A new model reduction method for the linear dynamic systems and its application for the design of compensator, *Circuits, Systems, and Signal Processing*, 39(5), 2328-2348. doi:10.1007/s00034-019-01264-1
26. Rahimian, M. A. and Tavazoei, M. S. (2012) Application of stability region centroids in robust PI stabilization of a class of second-order systems, *Transactions of the Institute of Measurement and Control*, 34(4), 487-498. doi:10.1177/0142331211400117
27. Sikander, A. and Prasad, R. (2017) A new technique for reduced-order modelling of linear time-invariant system, *IETE Journal of Research*, 63(3), 316-324. doi:10.1080/03772063.2016.1272436
28. Sinha, A. and Pal, J. (1990) Simulation based reduced order modelling using a clustering technique, *Computers & Electrical Engineering*, 16(3), 159-169. doi:10.1016/0045-7906(90)90020-G
29. Tan, N. (2005) Computation of stabilizing PI and PID controllers for processes with time delay, *ISA transactions*, 44(2), 213-223. doi:10.1016/s0019-0578(07)90000-2
30. Tan, N., Kaya, I., Yeroglu, C. and Atherton, D. P. (2006) Computation of stabilizing PI and PID controllers using the stability boundary locus, *Energy Conversion and management*, 47(18-19), 3045-3058. doi:10.1016/j.enconman.2006.03.022
31. Tyreus, B. D. and Luyben, W. L. (1992) Tuning PI controllers for integrator/dead time processes, *Industrial & Engineering Chemistry Research*, 31(11), 2625-2628. doi:10.1021/ie00011a029
32. Zhong, Q.-C. (2006) *Robust control of time-delay systems*, London: Springer. doi:10.1007/1-84628-265-9
33. Ziegler, J. G. and Nichols, N. B. (1942) Optimum settings for automatic controllers, *trans. ASME*, 64(11). doi:10.1115/1.4019264